

6-2013

Polymer Fiber Arrays for Adhesion

Shing Chung Josh Wong

University of Akron Main Campus, swong@uakron.edu

Johnny F. Najem

University of Akron Main Campus

Guang Ji

University of Akron, main campus

Shuwen Chen

Please take a moment to share how this work helps you [through this survey](#). Your feedback will be important as we plan further development of our repository.

Follow this and additional works at: http://ideaexchange.uakron.edu/mechanical_ideas



Part of the [Mechanical Engineering Commons](#)

Recommended Citation

Wong, Shing Chung Josh; Najem, Johnny F.; Ji, Guang; and Chen, Shuwen, "Polymer Fiber Arrays for Adhesion" (2013). *Mechanical Engineering Faculty Research*. 676.

http://ideaexchange.uakron.edu/mechanical_ideas/676

This Conference Proceeding is brought to you for free and open access by Mechanical Engineering Department at IdeaExchange@UAkron, the institutional repository of The University of Akron in Akron, Ohio, USA. It has been accepted for inclusion in Mechanical Engineering Faculty Research by an authorized administrator of IdeaExchange@UAkron. For more information, please contact mjon@uakron.edu, uapress@uakron.edu.

Polymeric Fiber Arrays for Adhesion

Shing-Chung Wong^{*}, Johnny F. Najem, Guang Ji, Shuwen Chen

Department of Mechanical Engineering, The University of Akron, Akron, OH 44325-3903

^{*} Corresponding author: swong@uakron.edu

Abstract The ability of geckos to adhere to vertical solid surfaces comes from their remarkable feet with millions of projections terminating in nanometer spatulae. In this paper, we present a simple yet robust method for fabricating directionally sensitive dry adhesives. By using electrospun nylon 6 nanofiber arrays, we create gecko-inspired dry adhesives, that are electrically insulating, and that show shear adhesion strength of 27 N/cm^2 on a glass slide. This measured value is 270% that reported of gecko feet and 97-fold above normal adhesion strength of the same arrays. The data indicate a strong shear binding-on and easy normal lifting-off. Size and surface boundary of fibers both affect on the shear adhesion. This anisotropic strength distribution is attributed to enhanced shear adhesion strength with decreasing fiber diameter and an optimum performance of nanofiber arrays in the shear direction over a specific range of thicknesses.

Keywords dry adhesion, high aspect ratio structure, electrospun nylon 6 nanofibers

1. Introduction

Geckos are exceptional in their ability to climb on smooth and rough surfaces. The feet of a gecko possess the most versatile adhesive known in nature which produces a clinging capability of 10 N/cm^2 [1]. With growing interest in detachable adhesives, new materials are explored such as the types that employ elastomers, thermoplastics, and pressure-sensitive polymers [2]. Generally, these adhesives produce substantial shear adhesion strengths but are considerably difficult to detach from surfaces. Commercial high strength adhesives make use of chemical interactions such as glues and permanently attach two surfaces. Subsequently, fabrication of dry adhesives with anisotropic force distributions has the potential in several applications such as tapes, fasteners, treads of wall-climbing robots, spiderman's suits, microelectronics, medical and space applications.

There are obvious size effects when the scaling decreases to nanoscale. High aspect ratio (AR) structures exhibit significant shear adhesion strength compared to ones with low AR(s) [3,4]. Electrospinning presents a versatile technique for fabricating nanofibers with significant AR [5,6]. Little has been done for fabricating dry adhesives, which are electrically insulating, and which possess significant shear adhesion strength with easy normal detachment.

With use of electrospun nylon 6 nanofiber membrane, we report herein the fabrication of electrically insulating dry adhesives with high shear adhesion strength for strong shear binding-on but with substantial normal detachment strength (V) for easy normal lifting-off. With the aid of microscopy and microanalyses, we investigate the effects of the fiber diameter, fiber surface roughness, and thickness of membrane on their corresponding adhesion strengths. Our research group first measured the adhesion work of electrospun polymer fibers [7-9] and, in this paper, we will focus on the bending stiffness and dimensional characteristics of these fiber fabrics. In our

study, we found that the stiffness of fiber fabrics and dimensional characteristics play a critical role in optimizing the van der Waals (vdW) interactions and thus the shear adhesion strength between electrospun nylon 6 and surface asperities.

2. Experimental

2.1. Collection of aligned electrospun fibers

Nylon 6 pellets (Sigma Aldrich, CAS 25038-54-4) are dissolved in formic acid (EMD Corporation, CAS 64-18-6) and magnetically stirred overnight. A syringe pump is employed for maintaining a solution drop on the tip of a stainless steel needle (Gauge 24). The latter needle is attached to a 5 mL capacity syringe filled with the solution. The needle is charged with a high voltage of 25 kV. The gap distance between the tip of the needle and the top of rotating disc collector is set to be 150 mm. Collector has a diameter of 150 mm and electrospun fibers are collected at take-up velocity of 20 m/s.

2.2. Fabrication of high AR nanofiber membrane

After collecting electrospun fibers for 10 minutes, a portion of the membrane is discarded to prepare the surface of the collector for peeling. A small part of the membrane is then placed on a glass slide using the tapered tip of a needle. The glass slide is thereafter rotated in the plane where membranes overlap one another. Subsequently, membranes with substantial thickness are obtained. These membranes are then installed in a holder.

2.3. Atomic Force Microscopy (AFM)

Contact-mode AFM is performed for investigating the elastic modulus of fiber E. A contact-mode probe (Veeco Inc.), with a tip radius of 12 nm and a cantilever spring constant of 0.125 N/m, is employed. The diameter and surface roughness of fibers are determined using tapping-mode AFM. A tapping-mode probe (MikroMasch Inc.), with a tip radius of 10 nm and a cantilever spring constant of 40 N/m, is employed. Scanning is done at a frequency of 0.5 Hz and data are analyzed by employing SPI3800N probe station software (Seiko, Inc.). Surface roughness of the nanofiber is obtained by tracing a line along the fiber axis. An average roughness of the fiber surface is determined.

2.4. Macroscopic adhesion testing

Nanofiber membrane is finger-pressed on a glass slide and then the weight is added to the end of the line. The weight consists of a beaker which is incrementally filled with water until membranes get separated from the glass slide. The contact area between membrane and a glass slide has a width and a length of 3 mm and 2 mm, respectively. The only two parameters which vary are membrane thickness and nanofiber diameter. No external normal load is applied to the membrane while being tested.

3. Results and discussion

3.1. Effects of membrane thickness (T) on shear adhesion

As shown in Figure 1A, nanofiber membrane displays low shear adhesion strengths for T less than 12 μm . However, for T ranging between 15 μm and 40 μm , the shear adhesion strength of nanofiber arrays substantially increases with rising T and reaches peak values. For T greater than 40 μm , the shear adhesion strength of membrane is significantly reduced with increasing T and reaches considerably low values above T of 80 μm . Shear adhesion testing is performed at an angle θ of 0° with the glass slide. The highest shear adhesion strength of 27 N/cm^2 is reached for membranes having fibers with d of 50 nm and T of 30 - 40 μm . A glass beaker is filled with water (total weight of 170 g, shear adhesion strength of 28.3 N/cm^2) and carried by a small piece of membrane (3 mm by 2 mm). This shear adhesion strength is 415% greater than the one reported for PC nanofiber-based dry adhesives [10]. As shown in Figure 1B, nanofibrous membranes may be considerably flexible with a weak tensile strength for T less than 12 μm . Subsequently, these membranes are expected to retain a minimal real contact area with a substrate. Thus, the latter membranes have limited vdW interactions and hence could not carry a heavy load. Nevertheless, as presented in Figure 1C, it is suggested that the flexibility and tensile strength of membranes reach optimum performances for T between 30 and 40 μm . Thus, membranes retain a significant real contact area with the glass substrate during loading, which leads to a substantial shear adhesion strength. However, as shown in Figure 1D, it is proposed that nanofibrous membranes start losing their flexibility for T greater than 40 μm . This phenomenon causes an extensive decrease in the real contact area between the fibers and the glass slide leading to deteriorating shear adhesion strength.

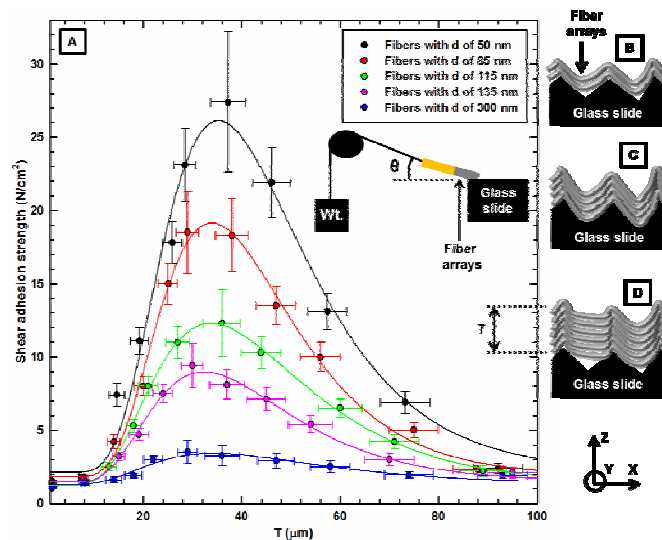


Figure 1. Shear adhesion strength as a function of T for aligned fiber membranes attached onto a glass slide with a preloading of 2kg

3.2. Effects of fiber packing density, nanofiber diameter (d) and fiber surface roughness on adhesion

As shown in Figure 2A-E, the packing density and aspect ratio of fibers are both noticeably enhanced with decreasing d . This enhancement is suggested to augment vdW interactions between

the fibers and the substrate leading to an upsurge in shear adhesion strength. As shown in Figure 2F, d extensively diminishes with decreasing concentration of polymer solution (R). The fiber packing density is characterized via SEM (FEI Quanta 200). Theoretical studies have shown that significant adhesion could be obtained by size reduction. Furthermore, the side contact of fibers with a substrate over a large contact area causes significant adhesion.

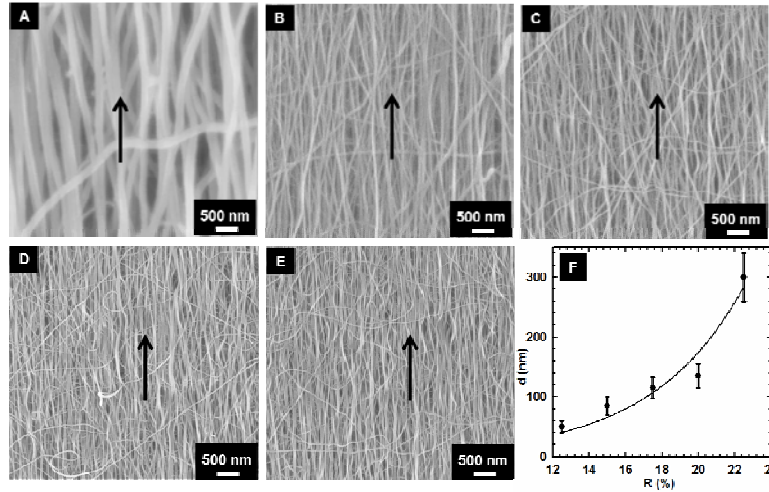


Figure 2. (A-E) Scanning electron microscopy (SEM) images of electrospun nylon 6 fibers with different d (s): 300 nm, 135 nm, 115 nm, 85 nm, and 50 nm, respectively; (F) d as a function of R

Surface boundary of fibers also makes contribution to the shear adhesion. For side wall contacts of fibers, the attractive force per unit length between the nanofiber and substrate is:

$$F_v = A\sqrt{d}/(16D^{2.5}) \quad (1)$$

Where A is the Hamaker constant, and D the gap distance between the surface of the nanofiber and the substrate [11,12]. There exists a cut-off gap distance $D=D_0$ which represents the effective separation between the nanofiber and substrate and at which the maximum F_v (F_{vM}) is estimated. The total F_{vM} is:

$$F_{vMK} = NLA\sqrt{d}/(16D_0^{2.5}) \quad (2)$$

Where N represents the total number of fibers along the contact width between the nanofiber arrays and the substrate (W) and is $N = W/d$. Replacing the value of N in the previous equation, we obtain:

$$F_{vMK} = LWA/(16D_0^{2.5}\sqrt{d}) \quad (3)$$

For constant values of W and the contact length between the nanofiber arrays and the substrate (L), F_{vMK} radically increases with decreasing d . These results suggest a substantial increase in the shear adhesion strength with diminishing d .

As shown in Figure 3, the surface roughness of fibers considerably diminishes with decreasing d . The latter decrease leads to a significant enhancement in shear adhesion strength between membrane and a substrate due to a considerable proliferation in the effective contact area.

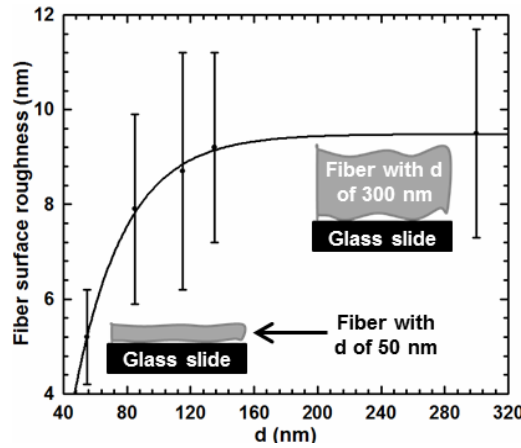


Figure 3. The surface roughness of a nanofiber as a function of d

3.3. Normal adhesion force

Membranes are easily peeled off a glass slide for $\theta = 90^\circ$. For a contact area of $(3 \times 2) \text{ mm}^2$ with a glass slide, the normal adhesion force of the membranes is roughly 0.015 N, regardless of d and T . Meanwhile, the maximum shear adhesion force for nanofiber arrays is 1.6 N (Fibers with d of 50 nm) which leads to a $V = 100$. Thus, these nylon 6 fiber membranes are 10 times easier to detach from a glass slide in the normal direction dry adhesives. This significant V value is suggested to be due to the high AR of the nanofibers in this work. Thus, a significant decrease in the effective contact area between the nanofibers and the substrate arises during vertical detachment, which leads to an easy normal lifting-off.

3.4. Effect of Nanofiber Bending Stiffness on Adhesion

The bending stiffness of a nanofiber is $b = EI$ where I is the moment of inertia of the cross section of a nanofiber [13]. The indentation of a cantilever tip into the nanofiber is directly proportional to lateral deflection of the cantilever (ΔX) [2]. According to the Hertz model, ΔX is defined as:

$$h = [2(1 - \nu^2)f / 4a^{0.5}E]^{2/3} \quad (4)$$

Where a is the AFM probe tip radius, ν the Poisson's ratio of the tested material, and f the applied normal load on a fiber. f is directly proportional to a sinusoidal drive signal (λ). As shown in Figure 4, ΔX continuously rises with increasing λ . Fibers with d of 300 nm display the largest slope (P). Fibers with d of 50 nm possess the smallest P where the latter is directly proportional to E . P of fibers with d of 300 nm (P_0) is taken as a reference value for determining the relative modulus of a fiber:

$$E_r = P/P_0 \quad (5)$$

As shown in Figure 5A, E_r for fibers with d of 50 nm is 6-fold above the one for fibers with d of 300 nm. This upsurge is mainly caused by the increase in molecular orientation during

electrospinning and nanofiber collection when d diminishes. Thus, it becomes more difficult for the tip of an AFM probe to penetrate deeper in the polymer chains of a fiber leading to a smaller ΔX value for a specific λ value [2]. Assuming that a nanofiber has a circular cross section [13],

$$I = \pi d^4 / 64 \quad (6)$$

The relative moment of inertia is:

$$I_r = I / I_0 = (d / d_0)^4 \quad (7)$$

Where d_0 is 300 nm and I_0 is I for d_0 . The relative bending stiffness is:

$$b_r = E_r I_r \quad (8)$$

And thus:

$$b_r = E_r (d / d_0)^4 \quad (9)$$

As shown in Figure 5B, $1/b_r$ significantly rises with decreasing d for fibers with d less than 120 nm. Fibers with d of 50 nm are 150 times more flexible than the ones with d of 300 nm. As shown in insets of Figure 5B, this noteworthy flexibility is suggested to cause a substantial enhancement in the real contact area between a nanofiber and a glass slide. This enhancement could play a critical role to significantly increase the shear adhesion strength between a nanofiber and a glass slide.

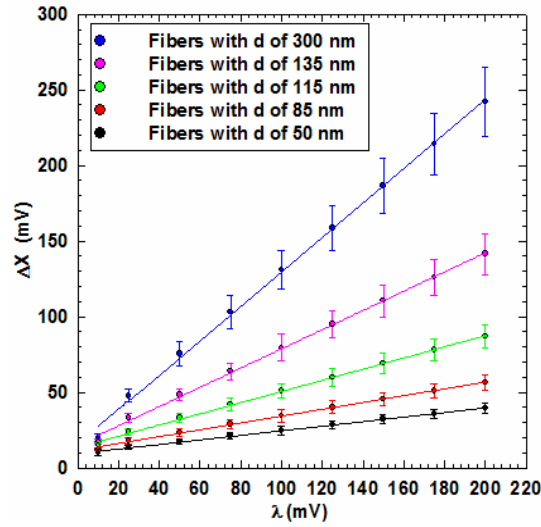


Figure 4. ΔX as a function of λ for fibers with varying d

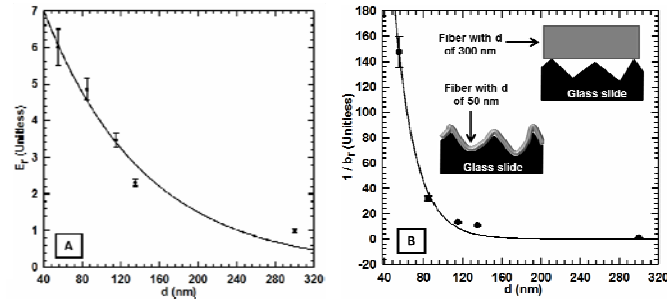


Figure 5. (A) E_r as a function of d . (B) $1/b_r$ as a function of d

4. Conclusions

We presented a technique for fabricating electrically insulating dry adhesives from electrospun nylon 6 nanofibers. These adhesives possess shear adhesion strength as high as 27 N/cm^2 on a glass slide. This measured value is 97-fold above normal adhesion strength of the same adhesive. For a definite d , the shear adhesion strength of membranes reaches optimum values for a specific range of arrays thicknesses while deteriorating otherwise. These optimum values suggest that these arrays could retain a significant real contact area with the substrate during loading. Fiber bending stiffness and fiber packing density are significantly increased with decreasing d while fiber surface roughness is noticeably reduced. These enhancements are proposed to considerably increase the shear adhesion strength between a nanofibrous membrane and a glass slide. The drastic increase is mainly attributed to a sizeable proliferation in vdW forces with enhanced contact area. This finding enables us to create electrically insulating dry adhesives with a strong shear adhesion and relatively weak normal adhesion for easy detachment.

Acknowledgements

This work is supported by National Science Foundation awards to SCW under CMMI 0746703 and IIP 1246773.

References

- [1] Autumn, K.; Dittmore, A.; Santos, D.; Spenko, M.; Cutkosky, M. Frictional, the Journal of Experimental Biology. 209 (2006), pp. 3569-3579.
- [2] Y Ji, C Li, G Wang, J Koo, S Ge, B Li, J Jiang, B Herzberg, T Klein, S Chen, J Sokolov, M Rafailovich, Euro Physics Letters (EPL), 84 (2008), pp.1-5.
- [3] C Greiner, A DelCampo, E Arzt, Langmuir, 23 (2007), pp. 3495-3502.
- [4] B Aksak, M Murphy, M Sitti, Langmuir, 23 (2007), pp. 3322-3332.
- [5] M Jose, B Steinert, V Thomas, D Dean, M Abdalla, G Price, G Janowski, Polymer, 48 (2007), pp. 1096-1104.
- [6] S-C Wong, A Baji, S Leng, Polymer, 49 (2008), pp. 4713-4722.
- [7] Q. Shi, K.-T. Wan, S.-C. Wong, P. Chen, T.A. Blackledge, Langmuir, 26 (2010), pp. 14188–14193.
- [8] H. Na, P. Chen, K.T. Wan, S.-C. Wong, Q. Li, Z. Ma, Langmuir 28 (2012) pp. 6677-6683 DOI: 10.1021/la300877r.
- [9] Q. Shi, S.-C. Wong, W. Ye, J. Hou, J. Zhao, J. Yin, Langmuir 28 (2012) pp. 4663-4671.
- [10] Ho A Yee, L Yeo, Y Lam, I Rodriguez, ACS Nano, 5 (2011), pp. 1897-1906.
- [11] Qu L., Dai L., Stone M., Xia Z., Wang Z., Science, 322 (2008), pp. 238-242.
- [12] Leckband, D.; Israelachvili, J. Quarterly Reviews of Biophysics, 34 (2001), pp. 105-267.
- [13] B Chen, P.D. Wu, H Gao, R.Soc. Proceeding of the Royal Society, Series A, 464 (2008), pp. 1639-1652.